High Absorption Contrast Quantum Confined Stark Effect in Ultra-Thin Ge/SiGe Quantum Well Stacks Grown on Si

Srinivasan Ashwyn Srinivasan, Clement Porret, Ewoud Vissers, Paola Favia, Jeroen De Coster, Hugo Bender, Roger Loo, Dries Van Thourhout, Joris Van Campenhout, and Marianna Pantouvaki

***Abstract*— We report on the performance of the quantum confined Stark effect (QCSE) in ultra-thin (~350 nm) Ge/SiGe quantum well stacks grown on Si. We demonstrate an absorption contrast Δα/α of 2.1 at 1 Vpp swing in QCSE stacks grown on ultra-thin (100 nm) strain relaxed GeSi buffer layers on 300 mm Si wafers. Such ultra-thin QCSE stacks will enable future integration of highly efficient QCSE electro-absorption modulators with low optical coupling loss to passive Si waveguides in a sub-micron silicon photonics platform.**

***Index Terms*— Germanium, stark effect, silicon photonics, optical interconnects.**

I. Introduction

SILICON photonics (SiPh) exploits the CMOS infrastructure and the associated economies of scale to realize active and passive devices and form complex photonics integrated circuits for short-reach interconnect applications [1]. Within SiPh platforms, Germanium has been widely used for photodetectors due to its direct band gap of 0.8 eV [2]. Electro-absorption modulators (EAM) exploiting the Franz-Keldysh effect (FKE) in Ge and GeSi have also enabled >50 Gbps NRZ-OOK and PAM4 modulation in the C and L band of fiber optic communication [2]–[4]. Combined with the high-density routing unctionality of sub-micron Si waveguides, GeSi EAM modulator arrays have shown great potential for realizing ultra-dense Terabit-scale SiPh transceivers in a fottprint of just a few mm^2 [5].

However, these FKE EAM modulators typically have a relatively high insertion loss (IL) for a targetted extinction ratio (ER) and suffer from relatively low figure of merit defined as FoM = ER/IL ~ 1-1.2 as a result of indirect bandgap of Ge(Si). To improve the modulator FoM, EAMs using Ge/GeSi multiple-quantum wells (MQW) have been considered as a promising alternative, by increasing the dynamic ER due to strong excitonic absorption peaks [6]. Demonstrations with such MQW stack have shown record absorption constrasts $\Delta\alpha/\alpha$ of 2.5 for 1 Vpp swing, operating at 1425-1575 nm wavelengths. Such MQW stacks can also be designed to operate in the O-band, making them an attractive option for intra-data center optical interconnect applications [7], [8]. An additional interesting feature is that the operation wavelength of these stacks can be tuned by the applied bias, as demonstrated by *Edwards et. al* [7]. As a result, the grown structures can potentially operate across a wide range of wavelengths without requiring thermal control.

However, the integration of the such relatively complex material stacks in a SiPh platform poses several – often conflicting – challenges. These include: (1) growing strain relaxed buffer (SRB) GeSi layers, (2) growing high-quality strain balanced multi-quantum wells and barriers on top of the SRB, (3) maximizing the electric field confinement in the wells by doping the buffer and top contact layers and (4) low optical coupling loss to the passive Si waveguides. Over the past years, various options have been explored to pursue the optimum trade-off. For example, several groups have reported on the use of thick SiGe (8-13 μm) virtual substrates (VS) [8], [9], to grow MQW stacks on buffer layers with relatively low threading dislocation densities. However, such thick buffers pose difficulties in coupling light to and from SOI waveguides (WG). These limitations typically require the implementation of a dedicated, specialty Ge-based photonic platform [9]. Alternatively, the growth of MQW stacks on 0.3 μm thick buffer layers to fabricate devices with a total thickness of ~0.65 μm has also been demonstrated [7]. This design allows for an efficient evanescent coupling with the SOI WG through

Manuscript received August 13, 2019; revised October 15, 2019; accepted October 20, 2019. Date of publication October 25, 2019; date of current version December 3, 2019. This work was supported by the imec's Industry-Affiliation Program on Optical I/O. *(Srinivasan Ashwyn Srinivasan, Clement Porret, and Ewoud Vissers contributed equally to this work.) (Corresponding author: Srinivasan Ashwyn Srinivasan.)*

S. A. Srinivasan, J. De Coster, J. Van Campenhout, and M. Pantouvaki are with the 3D and Silicon Photonics Technologies Department, Interuniversity Microelectronics Center, 3001 Leuven, Belgium (e-mail: ashwyn.srinivasan@imec.be; jeroen.decoster@imec.be; joris.vancampenhout@imec.be; marianna.pantouvaki@imec.be).

C. Porret and R. Loo are with the Epitaxial Growth Group, Interuniversity Microelectronics Center, 3001 Leuven, Belgium (e-mail: clement.porret@imec.be; roger.loo@imec.be).

E. Vissers was with the 3D and Silicon Photonics Technologies Department, Interuniversity Microelectronics Center, 3001 Leuven, Belgium. He is now with the Photonics Research Group, Department of Information Technology, Ghent University–imec, 9052 Ghent, Belgium (e-mail: ewoud.vissers@ugent.be).

P. Favia and H. Bender are with the Materials and Components Analysis Department, Interuniversity Microelectronics Center, 3001 Leuven, Belgium (e-mail: paola.favia@imec.be; hugo.bender@imec.be).

D. Van Thourhout is with the Photonics Research Group, Department of Information Technology, Ghent University–imec, 9052 Ghent, Belgium (e-mail: dries.vanthourhout@ugent.be).

Color versions of one or more of the figures in this article are available online at http://ieeexplore.ieee.org.

Digital Object Identifier 10.1109/JQE.2019.2949640

0018-9197 © 2019 IEEE. Personal use is permitted, but republication/redistribution requires IEEE permission.
See http://www.ieee.org/publications_standards/publications/rights/index.html for more information.

Authorized licensed use limited to: University of Gent. Downloaded on March 09,2020 at 15:00:11 UTC from IEEE Xplore. Restrictions apply.

TABLE I
BUFFER DETAILS FOR THE FABRICATION OF THE STACKS INVESTIGATED IN THIS WORK

Stack	Epitaxy strategy	Thickness	Doping
A	Epi + Anneal + CMP	0.6 µm	Undoped
B	Epi + Anneal + CMP	0.2 µm	Undoped
C	Epi + Anneal	0.2 µm	p-type
D	Epi + Anneal	0.15 µm	p-type
E	Epi + Anneal	0.1 µm	p-type

an adiabatic 3D taper but increases the process complexity for horizontal and/or vertical taper structures [10]. Thinning the buffer layer further would enable butt-coupling schemes like used in GeSi FKE EAMs with typical coupling loss of <1 dB and would allow the integration of such complex stacks in existing SiPh platforms [11]. With this motivation, we report on the growth and performance of MQW stacks on ultra-thin buffer layers with a thickness down to 100 nm (thinnest to date). As will be shown, reducing the buffer layer thickness introduces additional linewidth broadening to the excitonic absorption spectrum, most likely due to increased defect density. The impact of this broadening on the absorption contrast ($\Delta\alpha/\alpha$) associated with Stark effect will be investigated in this paper. The resulting total device thickness of ~0.4 μm is comparable to that of Ge based FKE EAMs and enables the future integration of QCSE EAMs in a sub-micron SiPh platform.

II. MATERIAL GROWTH AND DEVICE FABRICATION

The MQW stacks investigated in this work rely on an epitaxial growth strategy that minimizes strain build-up through the stack grown atop a buffer layer [7]. Ge QWs with a thickness of 14 nm were sandwiched between 18 nm thick $Si_{0:19}Ge_{0:81}$ barrier layers and grown on top of $Si_{0:11}Ge_{0:89}$ strain-relaxed buffers. Five different stacks with varying buffer thickness are investigated in this paper. Details corresponding to each of them are summarized in Table I. Si (001) substrates (300 mm) were first ion-implanted with B (active doping level of $\sim 3\times10^{18}$ cm^{-3}) to form a p-doped bottom contact. The wafers were then cleaned and dipped in HF prior to being loaded in a reduced pressure chemical vapor deposition production cluster (ASM-Intrepid XP^{TM}). After a short pre-epi bake at 850 °C, buffer layers were grown using conventional Ge and Si precursors, GeH_4 and SiH_2Cl_2, respectively. In stacks A and B, the buffer was first grown to a target thickness of 1 μm, annealed at 850 °C for 3 minutes and chemical mechanically polished down to the desired thickness as listed in Table I. The buffers used in stacks C, D and E were directly grown to the targeted thickness and then annealed. The anneal is intended to reduce the density of threading dislocations originating from strain relaxation at the ~3.7 % mismatched Si/SiGe interface [12]. For stacks A and B, since the anneal was performed after the growth of the 1 μm $Si_{0:11}Ge_{0:89}$ buffer layer and before the CMP step, the threading dislocation density (TDD) was measured to be 2.3×10^8 cm^{-2} [12]. This approach provides the lowest

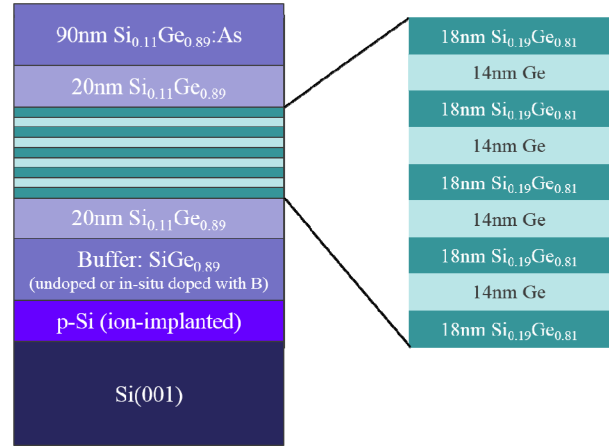

Fig. 1. Schematic elaborating the stack design used for the Ge/SiGe quantum wells targeted to be grown on Si [7]. The thickness and the epitaxy strategy used for growing the buffer are described in Table I.

TDD amongst all stacks, but it increases process complexity due to the additional CMP step. On the other hand, buffers used for stacks C, D and E exploit the CMP-free approach and were in-situ doped with B (using diborane, B_2H_6) during epi with an active doping level of $\sim 3\times10^{18}$ cm^{-3}. Doping the buffer helps in confining the applied electric bias to the MQW located in the intrinsic region of the diode. However, due to the reduced buffer thickness and the absence of the CMP step, the defect density and surface roughness are expected to be higher in Stack C to E. This will introduce additional linewidth broadening to the excitonic absorption spectrum. The impact of this broadening on device performance is investigated in this paper.

The quantum well stacks, used for this study are schematically shown in Fig. 1. They were grown at low temperature (350 °C) to limit the risk of SiGe interdiffusion between the different layers. Growth rates of 5-6 nm/min with accurate process control were possible at this reduced temperature due to the combination of digermane (Ge_2H_6) and disilane (Si_2H_6) as Ge and Si precursors, respectively. Following the deposition of the MQW, a 20 nm thick undoped $Si_{0:11}Ge_{0:89}$ capping layer and a 90 nm thick n-type in-situ doped $Si_{0:11}Ge_{0:89}$:As top contact layer was deposited. Arsine (AsH_3) was used for the in-situ doping of the top layer to form the n-contact of the diode. A chemical concentration of $\sim 1\times10^{19}$ cm^{-3} was obtained by SIMS.

X-ray diffraction (XRD), Atomic Force Microscopy (AFM) and Electron Channeling Contrast Imaging (ECCI) were first used to estimate strain in the buffer layers, to compare samples morphology and to estimate the resulting TDD for the different stacks [13]. Some of these characteristics are summarized in Table II. Secondary ion mass spectroscopy (SIMS, not shown here), transmission electron microscopy (TEM), energy-dispersive X-ray spectroscopy (EDS) and nano-beam diffraction (NBD) were then combined to characterize the compositions, strain levels and structural properties of the different stacks. Figure 2 shows cross-sectional TEM image, EDS and NBD data corresponding to stack E. Fig. 2(a)

Authorized licensed use limited to: University of Gent. Downloaded on March 09,2020 at 15:00:11 UTC from IEEE Xplore. Restrictions apply.

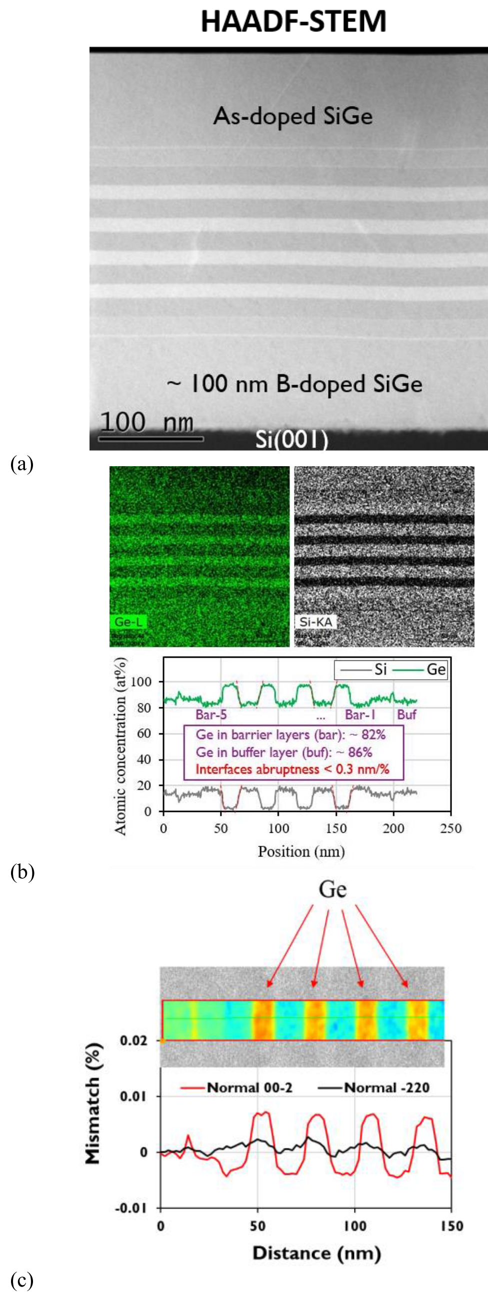

Fig. 2. (a) Cross-sectional transmission electron micrograph (TEM) image, (b) energy-dispersive X-ray spectroscopy data, and (c) nano-beam diffraction measurements performed across the MQW region in stack E. The presented set of data confirms the presence of the 100% strain relaxed buffer and fully strained MQW region with chemical composition.

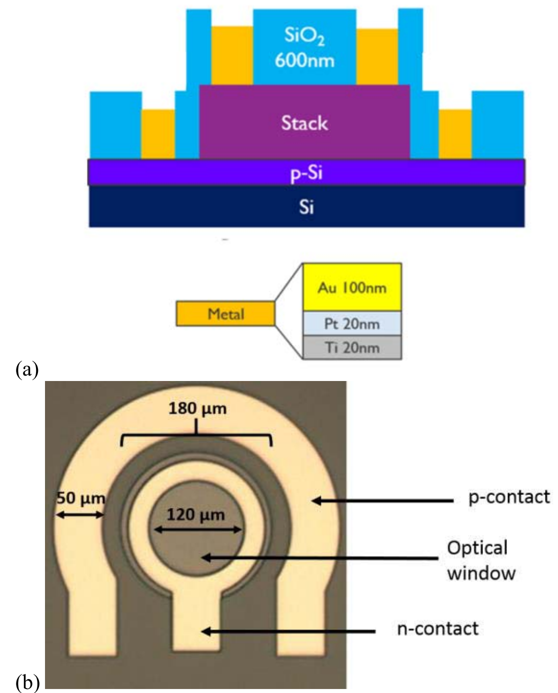

Fig. 3. (a) Cross-sectional schematic and (b) top-view micrograph image of a fabricated diode used for photocurrent measurements.

TABLE II
CHARACTERIZATION DETAILS FOR STACKS A TO E

Stack	Buffer strain Relaxation (%)	roughness across 40×40 μm^2	QCSE stack TDD (cm^{-3})
A	105	0.9 nm	~2.3×10^8
B	105	1.1 nm	~3.6×10^8
C	105	4.2 nm	~1.0×10^9
D	106	NA	NA
E	106	NA	NA

confirms the presence of very sharp MQW interfaces (interface abruptness < 0.3 nm/%) and a good thickness control for the different layers constituting the stack. Si concentration of 14% and 18% were measured in the buffer and barrier layers, respectively, by SIMS and EDS as can be seen in Fig. 2(b), while the nominal Si composition we targeted were 11% and 19%. XRD and NBD (Fig. 2(c)) confirmed the presence of fully strained-balanced layers grown on top of fully relaxed buffers. In addition, SIMS and EDS data indicated very limited Ge-Si interdiffusion between the different layers across the entire stack.

To quantify the quantum confined Stark effect-based electro absorption, the absorption spectrum of these stacks was measured under the influence of an external bias. This was accomplished by monitoring the photocurrent spectrum generated in the diode as function of applied electric field [6]–[9]. To facilitate these measurements, test p-i-n diodes were fabricated with the MQW region located in the intrinsic region of the diode [11]. Ge/SiGe MQW stacks were first vertically dry etched down to the Si substrate to form circular mesa structures and then covered with SiO_2 to provide electrical isolation. Ti/Pt/Au contacts with circular openings at the center of the device were defined using electron beam evaporation and a subsequent lift-off process. The resulting diodes were subsequently illuminated using a tunable laser equipped with a cleaved SMF-28 fiber. A top-view microscope image and the cross-sectional schematic of the fabricated devices can be found in Fig. 3 [11], [14].

Authorized licensed use limited to: University of Gent. Downloaded on March 09,2020 at 15:00:11 UTC from IEEE Xplore. Restrictions apply.

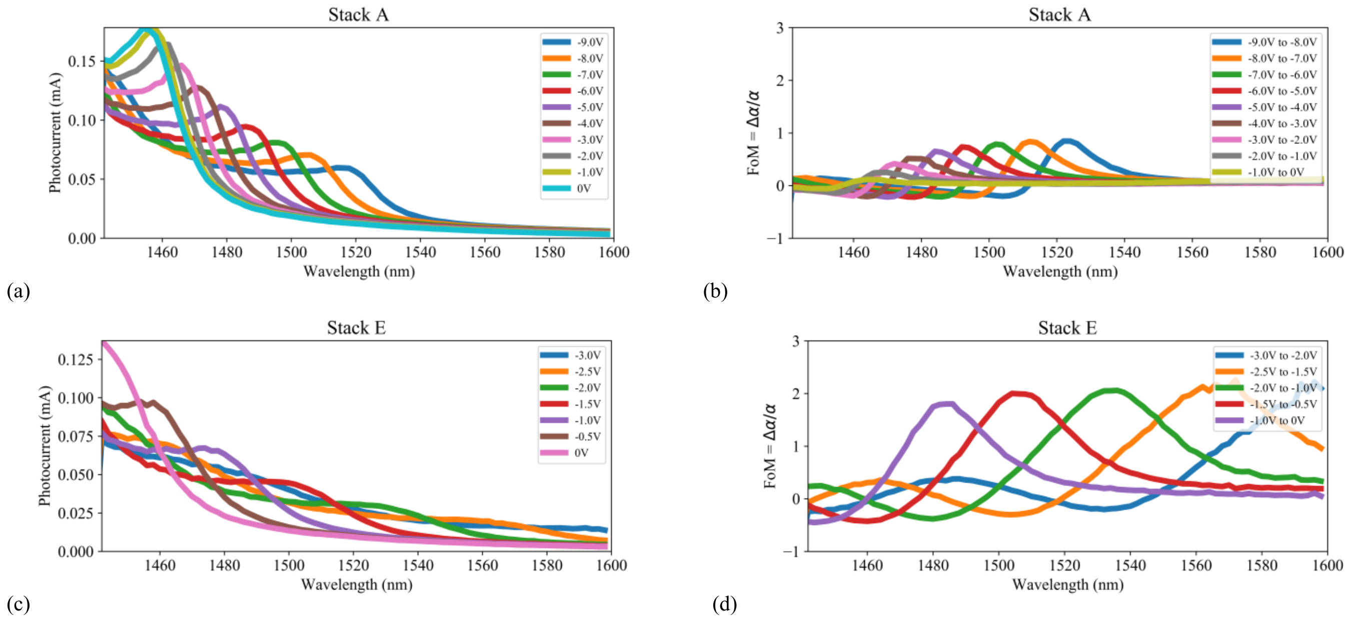

Fig. 4. Photocurrent spectra and the corresponding absorption contrast ($\Delta\alpha/\alpha$) for 1 V swing of the surface illuminated diodes fabricated with stack A and E as described in Table I. The photocurrent measurements were performed at 75 °C.

III. Device Measurement and Analysis

The absorption spectrum of each stack was first measured using a free-space spectrometer. Sharp absorption features corresponding to excitonic resonance around 1425 nm were observed at room temperature, in agreement with previous demonstration in literature [7], [14]. However, the tunable laser used for the photocurrent measurement only supports a wavelength range of 1440 – 1640 nm. For this reason, the devices were heated up to 75 °C to shift the absorption spectrum of the stack by $\sim$ 40 nm, due to the temperature dependent bandgap narrowing effect [3]. The measured photocurrent responses from devices using stack A and E are shown in Fig. 4. They were normalized by subtracting the measured dark current from the measured light current, even though the dark currents were at least two order of magnitude lower than the light current. Using TCAD simulations, the photo-excited carrier extraction quantum efficiency was estimated to be unity, confirming that the measured photocurrents provides a direct translation of optical absorption [6], [15]. Sharp absorption peaks at 0 V near 1460 nm wavelength correspond to the excitonic absorption associated with the lowest quantized transition energy in the quantum wells at 75 °C. With the application of an external bias, this transition energy is modulated resulting in a shift of the excitonic resonance wavelength in the photocurrent spectra as can be seen in Fig. 4. The peak photocurrent associated with this excitonic resonance drops with applied electric field due to the reduction of overlap integral between the electron and hole wavefunctions in the quantum well [6], [15], [16]. Absorption contrasts ($\Delta\alpha/\alpha$) for a voltage swing of 1 V swing and applied external bias were extracted from these photocurrent responses. Fig. 4 and Fig. 5 also show the result of the extracted absorption contrast ($\Delta\alpha/\alpha$). The peak $\Delta\alpha/\alpha$ extracted in stacks A and B for 1 V swing were lower than those of stacks C, D and E. This is explained by the presence of thick undoped buffer layers in the intrinsic region of the diode. As a result, the applied DC bias swing of 1 V does not effectively translate to a potential drop across the MQW region.

To compare the FoM from different stacks, the analysis is restricted to voltage swings with comparable electric field contrasts across the intrinsic region. To facilitate such a comparison, C-V measurements were first performed to estimate the diode intrinsic region width, built-in voltage and hence the effective electric field in each of the investigated stacks, similar to [15]. For a voltage swing of 0 to 1 V, the E-field varies from 6.3 to 19.8 kV/cm in stack A, 18.2 to 53.4 kV/cm in stack B and 31.2 to 89.2 kV/cm in stacks C, D and E. To compare the absorption contrast between the samples, the voltage swing has been rescaled such that the electric field experienced by the quantum well region remains the same. As a result, for an E-field contrast 58 kV/cm, a voltage swing from 0 V to 1 V for devices with stacks C, D and E corresponds to a voltage swing of 1.8 to 6.1 V in stack A and 0.4 to 2.0 V in stack B. The FoM spectra for stacks A (Fig. 5. a) and stack B (Fig. 5. b) were thereafter recalculated with the voltage scaling factor. The resulting peak of each FoM spectra and its full width half maxima (FWHM) were extracted and plotted against bias voltages as can be seen in Fig. 5 (c) to 5(h). Devices with stacks C, D and E have a peak FoM of 2.8, 2.6 and 2.1 for an E-field contrast of 58 kV/cm (or 1 V swing), whereas devices with stack A and B have a peak FoM 2.9 and 3.1 respectively. The reduction of FoM with decreasing buffer thickness is shown in Fig. 5. This reduction can be attributed to the broadening of the absorption spectrum as can be seen with the increase of the FoM's full width of half maxima (FWHM) with reduced buffer thickness. We believe that this increase in broadening is due to increased surface roughness and defect density in thin strain-relaxed buffer layer.

Authorized licensed use limited to: University of Gent. Downloaded on March 09,2020 at 15:00:11 UTC from IEEE Xplore. Restrictions apply.

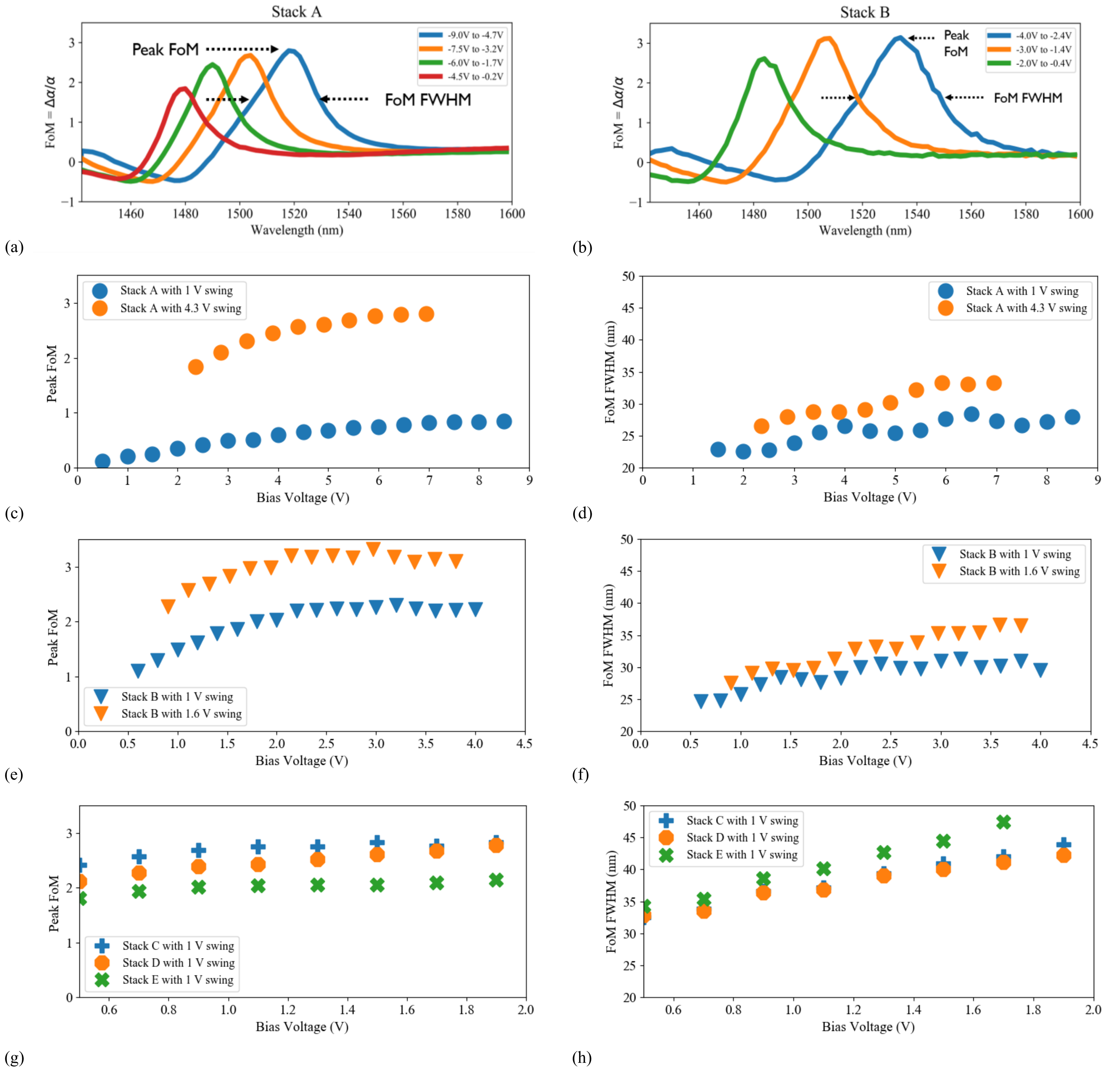

Fig. 5. The absorption contrast spectra with (a) 4.3 V swing for stack A and (b) 1.6 V swing for stack B, such that the E-field contrast in the multi-quantum well region is like that experienced by devices with stack C to E for 1 V swing. As indicated in (a) and (b), the extracted peak FoM and full width half maxima (FWHM) of each FoM spectrum for voltage swing against bias voltages have been plotted in (c) to (h).

IV. Benchmarking

The performance of the stacks presented in this work is compared with other state of the art Ge based electro absorption modulators in Table III. Even with the increased broadening as seen in Fig. 4, the devices made with stack D have similar absorption contrast as the previous start of the art device demonstration from *Edwards et. al* [7], achieved using a total stack thickness of ∼400 nm. Moreover, the low dark current densities measured with stacks A to E, as compared to other waveguide integrated devices presented by *Pantouvaki et. al* and *Srinivasan et. al*, indicate that they originate from the waveguide interfaces and not bulk defects [2], [3], [17], [18]. A final stack thickness of 350-400 nm makes stack D and E comparable to coupling schemes used in Ge based FKE electro-absorption modulators, integrated in imec's silicon photonics platform. While the results presented in this work were obtained from the photocurrent measurements, observation of modulation through transmission measurements is essential for these stacks as it includes the coupling loss between SOI waveguide and modulator, excess metal loss

Authorized licensed use limited to: University of Gent. Downloaded on March 09,2020 at 15:00:11 UTC from IEEE Xplore. Restrictions apply.

TABLE III
COMPARING THE DEVICE PERFORMANCE OF Ge/GeSi BASED QUANTUM CONFINED STARK EFFECT ELECTRO-ABSORPTION STACKS PRESENTED IN THIS WORK AND IN LITERATURE

Ref	Stack thickness (nm)	λ (nm)	V_{pp} (V)	FoM or $\Delta\alpha/\alpha$	Coupling method	Dark current at -1V (A/μm^2)
[8]	~ 1850	1385-1405	6	~2.3	Surface illuminated	NA
[7]	~ 614	1450-1575	1	~2.5	Surface illuminated	NA
Stack A	~ 900	1460-1530	4.3	2.9	Surface illuminated	7.6×10^{-12}
Stack B	~ 450	1460-1530	1.6	3.1	Surface illuminated	4×10^{-11}
Stack C	~ 450	1480-1600	1	2.8	Surface illuminated	5.8×10^{-12}
Stack D	~ 400	1480-1600	1	2.6	Surface illuminated	1.2×10^{-11}
Stack E	~ 350	1480-1600	1	2.1	Surface illuminated	2.2×10^{-11}

and the free-carrier absorption from the doped layers in the stack. Nevertheless, these stacks pave the way to have future waveguide integrated electro-absorption modulator demonstrations.

V. CONCLUSION

To summarize, a record absorption contrast ($\Delta\alpha/\alpha$) of 2.1 for 1 V swing is demonstrated in Ge/GeSi multi quantum wells grown on ~100 nm thick buffer layers. Stacks with varying buffer thicknesses and growth strategies were investigated to identify the impact of defects and surface roughness on the stack performance. By reducing the buffer thickness from 0.6 μm to 0.1 μm, the device FoM dropped from 3.1 to 2.1 due to linewidth broadening associated with the increased surface roughness and material defect density. Nevertheless, study with a buffer thickness of 100 to 150 nm still have $> 2\times$ higher FoM as compared to the current state-of-the-art Ge or GeSi based Franz-Keldysh effect electro-absorption modulators, without compromising on the total stack thickness. This result is promising for the future integration of waveguide integrated devices in a sub-micron silicon photonics platform.

ACKNOWLEDGMENT

Air Liquide Advanced Materials is acknowledged for providing Ge_2H_6.

REFERENCES

[1] D. A. B. Miller, "Device requirements for optical interconnects to silicon chips," *Proc. IEEE*, vol. 97, no. 7, pp. 1166–1185, Jul. 2009.

[2] M. Pantouvaki *et al.*, "Active components for 50 Gb/s NRZ-OOK optical interconnects in a silicon photonics platform," *J. Lightw. Technol.*, vol. 35, no. 4, pp. 631–638, Feb. 15, 2017.

[3] S. A. Srinivasan *et al.*, "56 Gb/s germanium waveguide electro-absorption modulator," *J. Lightw. Technol.*, vol. 34, no. 2, pp. 419–424, Jan. 15, 2016.

[4] J. Verbist *et al.*, "Real-time 100 Gb/s NRZ and EDB transmission with a GeSi electroabsorption modulator for short-reach optical interconnects," *J. Lightw. Technol.*, vol. 36, no. 1, pp. 90–96, Jan. 1, 2018.

[5] P. De Heyn *et al.*, "Ultra-dense 16×56 Gb/s NRZ GeSi EAM-PD arrays coupled to multicore fiber for short-reach 896 Gb/s optical links," in *Proc. Opt. Fiber Commun. Conf. Exhib. (OFC)*, Mar. 2017, pp. 1–3.

[6] Y.-H. Kuo *et al.*, "Strong quantum-confined Stark effect in germanium quantum-well structures on silicon," *Nature*, vol. 437, pp. 1334–1336, Oct. 2005.

[7] E. H. Edwards *et al.*, "Low-voltage broad-band electroabsorption from thin Ge/SiGe quantum wells epitaxially grown on silicon," in *Opt. Exp.*, vol. 21, pp. 867–876, 2013.

[8] M.-S. Rouifed *et al.*, "Advances toward Ge/SiGe quantum-well waveguide modulators at 1.3 μm," *IEEE J. Sel. Topics Quantum Electron.*, vol. 20, no. 4, Jul./Aug. 2014, Art. no. 3400207.

[9] P. Chaisakul *et al.*, "Integrated germanium optical interconnects on silicon substrates," *Nature Photon.*, vol. 8, no. 6, pp. 482–488, 2019.

[10] K. Zang *et al.*, "Germanium quantum well QCSE waveguide modulator with tapered coupling in distributed modulator–detector system," *J. Lightw. Technol.*, vol. 35, no. 21, pp. 4629–4633, Nov. 1, 2017.

[11] S. A. Srinivasan *et al.*, "High-contrast quantum-confined stark effect in Ge/SiGe quantum well stacks on Si with ultra-thin buffer layers," in *Proc. CLEO Pacific Rim Conf.*, Jul./Aug. 2018, pp. 1–2.

[12] G. Wang *et al.*, "A model of threading dislocation density in strain-relaxed Ge and GaAs epitaxial films on Si (100)," *Appl. Phys. Lett.*, vol. 94, no. 10, 2009, Art. no. 102115.

[13] A. Schulze *et al.*, "Non-destructive characterization of extended crystalline defects in confined semiconductor device structures," *Nanoscale*, vol. 10, no. 15, pp. 7058–7066, 2018.

[14] S. A. Srinivasan, "Advanced germanium devices for optical interconnects," Ph.D. dissertation, Dept. Inf. Technol., Ghent Univ., Ghent, Belgium, 2018.

[15] R. K. Schaevitz, J. E. Roth, S. Ren, O. Fidaner, and D. A. B. Miller, "Material properties of Si-Ge/Ge quantum wells," *IEEE J. Sel. Topics Quantum Electron.*, vol. 14, no. 4, pp. 1082–1089, Jul. 2008.

[16] S. L. Chuang, *Physics of Photonic Devices*, vol. 80. Hoboken, NJ, USA: Wiley, 2012.

[17] H. Chen *et al.*, "Dark current analysis in high-speed germanium p-i-n waveguide photodetectors," *J. Appl. Phys.*, vol. 119, no. 21, 2016, Art. no. 213105.

[18] A. Leśniewska, S. A. Srinivasan, J. Van Campenhout, B. J. O'Sullivan, and K. Croes, "Accelerated device degradation of high-speed Ge waveguide photodetectors," in *Proc. IEEE Int. Rel. Phys. Symp.*, Mar./Apr. 2019, pp. 1–7.

Srinivasan Ashwyn Srinivasan received the master's degree in micro and nanotechnologies for integrated systems from the Swiss Federal Institute of Technology Lausanne, Lausanne, Switzerland, the Grenoble Institute of Technology, Grenoble, France, and the Politecnico di Torino, Turin, Italy, in 2013, with La Mention Tres Bien and 110/110 con lode, and the Ph.D. degree in advanced Ge devices for optical interconnect applications from the University of Ghent–imec, Ghent, Belgium, in 2018. He is currently an R&D Photonics Device and Integration Engineer with imec, working on next generation active photonic devices for improved optical link power efficiency and bandwidth density. His research interests include solving complex technological problems in the field of optics, communication, electronics, and quantum communication. He is a member of OSA.

Clement Porret received the Engineer degree in physics, with major in component physics, from the Grenoble Institute of Technology, the M.S. degree in micro and nanoelectronics from the University of Grenoble, France, in 2007, and the Ph.D. degree in material science from the University of Grenoble in 2011, with the focus on the growth of Mn-doped Ge nanostructures for spintronics applications. From 2011 to 2015, he was an R&D and a Process Engineer at Riber SA, a Molecular Beam Epitaxy (MBE) tool manufacturer, where he worked on III–V surface engineering and passivation, using a SEMI-compatible 300-mm MBE system connected to the state-of-the-art III–V CMOS Metal Organic Vapor Phase Epitaxy (MOVPE) production cluster. The project also included the deposition of high-K dielectric materials for future logic devices. In 2015, he joined imec as a SiGe Epitaxy Researcher, with the development of solutions for sub-14 nm technology nodes using Reduced-Pressure Chemical Vapor Deposition (RP-CVD) as a main task. Since then, he has been involved in various projects, including the formation of strained channels, the selective epitaxial growth of highly-doped source/drain materials for Si and Ge fin and gate-all-around field-effect transistors, the synthesis of graphene on Si compatible platforms, and the fabrication of integrated electro-absorption modulators.

Authorized licensed use limited to: University of Gent. Downloaded on March 09,2020 at 15:00:11 UTC from IEEE Xplore. Restrictions apply.

Ewoud Vissers received the M.Sc. degree in electrical engineering from the University of Twente, Enschede, The Netherlands, in 2018. He is currently pursuing the Ph.D. degree with the Photonics Research Group, Department of Information Technology, Ghent University–imec, Ghent, Belgium. During his M.Sc. degree, he participated in this work at the 3D and Silicon Photonics Technologies Department, imec, Leuven, Belgium.

Paola Favia received the Ph.D. degree in solid state physics from the Ecole Polytechnique Federale de Lausanne, Switzerland, in 1996. From 1997 to 2004, she was an R&D Researcher with Gatan Inc., Pleasanton, CA, USA. Since 2006, she has been with imec, Belgium, where she is currently a Senior Researcher. Her research interest includes applications of electron microscopy techniques to nano-electronic devices.

Jeroen De Coster received the master's degree in electrical power engineering and the Ph.D. degree in electrical engineering from KU Leuven, Leuven, Belgium, in 2001 and 2006, respectively, with focus on the design, modeling, and characterisation of RF-MEMS devices. Since 2006, he has been with imec, Belgium, working on the development of measurement tools and procedures for functional characterization, as well as yield and reliability testing–application areas of which are in MEMS, memory, and silicon photonics.

Hugo Bender is currently a Principal Member Technical Staff with the Materials and Components Analysis (MCA) Department, imec. He has more than 40 years of experience in materials characterization for semiconductor applications, in particular with transmission electron microscopy, scanning electron microscopy, focused ion beam, auger spectroscopy, spectroscopic ellipsometry, infrared spectroscopy, etc. In these fields, he is the author or coauthor of more than 300 journal articles, 500 conference contributions, and five book chapters. His current interests include materials analysis for advanced 3D semiconductor devices and beyond CMOS technologies focusing on transmission electron microscopy for strain analysis, electron and EDS tomography, MX2 materials, chemical analysis by STEM/EDS/EELS/ELNES and hybrid analysis combining TEM and Raman spectroscopy, and atom probe or SPM techniques.

Roger Loo received the master's degree in experimental physics and the Ph.D. degree from R. W. T. H., Aachen, Germany, in 1993 and 1997, respectively. In January 1997, he joined imec, Leuven, Belgium, where he is currently a Leading Principal Scientist for Group IV epi activities.

Dries Van Thourhout received the degree in physical engineering and the Ph.D. degree from Ghent University, Ghent, Belgium, in 1995 and 2000, respectively. From October 2000 to September 2002, he was with Lucent Technologies, Bell Laboratories, NJ, USA, working on the design, processing and characterization of InP/InGaAsP monolithically integrated devices. In October 2002, he joined the Department of Information Technology (INTEC), Ghent University. He is currently a member of the Permanent Staff of the Photonics Group as a full-time Professor. He is also working on applications for telecom, diatom, optical interconnect and sensing. His research interests include the design, fabrication, and characterization of integrated photonic devices. Main topics involve Silicon nanophotonic devices and the integration of novel materials (III–V, graphene, ferro-electrics, and quantum dots) on these waveguides to expand their functionality. He is also a member of the IEEE Photonics Society, OSA, and SPIE.

Joris Van Campenhout received the Ph.D. degree in electrical engineering from Ghent University, Belgium, in 2007, with the focus on heterogeneous integration of electrically driven III–V microdisk lasers on silicon photonic waveguide circuits. In 2010, he was a Post-Doctoral Researcher with IBM's T. J. Watson Research Center, NY, USA, where he developed silicon electro-optic switches for chip-level reconfigurable optical networks. He is currently the Chief Technologist in silicon photonics and the Director of the Optical I/O industry-affiliation R&D program with imec, which covers the development of a scalable and industrially viable short-reach optical interconnect technology through silicon photonics. He holds seven patents. He has authored or coauthored more than 100 articles in the field of silicon integrated photonics, which have received more than 7000 citations.

Marianna Pantouvaki received the Ph.D. degree in electronic and electrical engineering from University College London (UCL), London, U.K., in 2004 for her work on all-optical signal regeneration in high bit-rate long-distance optical fiber systems. From 2003 to 2006, she was a Research Fellow with the Ultra-Fast Photonics Group, UCL, while from 2004 to 2005, she was also a Visiting Researcher with the Centre for Integrated Photonics, Ipswich, U.K., focusing on the monolithic integration of InP-based DBR lasers and modulators. From 2006 to 2010, she was a BEOL Integration Engineer for the advanced Cu/low-k Interconnect Program, imec, Leuven, Belgium, where she worked on the development of high-speed silicon photonics transmitters and novel exploratory devices for optical interconnects from 2010 to 2015. She has been the Manager of the Optical IO Industrial Affiliation Program, imec, since 2016.

Authorized licensed use limited to: University of Gent. Downloaded on March 09,2020 at 15:00:11 UTC from IEEE Xplore. Restrictions apply.